Available online at www.rajournals.in

RA JOURNAL OF APPLIED RESEARCH
ISSN: 2394-6709
DOI:10.47191/rajar/v8i5.19
Volume: 08 Issue: 05 May -2022

International Open Access

Impact Factor- 7.108

Page no.- 422-430

Contaminant Crossover in Residential Energy Recovery Ventilators: Mass Spectrometric Analysis and Introducing Remediation Measures

Naveen Weerasekera[1], Ryan Martil[2], Dawa Ram Shingdan[3], Nethmini Weerasekera[4], Agnimitra Biswas[5], Siyua Cao[6]

[1]Department of Mechanical Engineering, University of Louisville, Louisville, KY, USA
[2]Department of Mechanical Engineering, Portland State University, Portland, OR, USA
[3]Department of Environmental Sciences Nagoya University, Aichi-Prefecture, Nagoya, JAPAN
[4]Department of Biochemistry and Molecular Biology, Oregon State University, Corvallis, OR, USA
[5]Department of Mechanical Engineering, National Institute of Technology Silchar, Assam, INDIA
[6]Department of Mathematics and Statistics, Portland State University, Portland, OR, USA

ARTICLE INFO

Published Online:
24 May 2022

Corresponding Author:
Siyua Cao

ABSTRACT

Energy recovery ventilators (ERV) are increasingly present in residential environments to enable energy-efficient provision of controlled outdoor air ventilation. In this work, we investigated pollutant transport through a typical residential ERV as a potential pathway for re-entrainment of indoor air pollutants into the outdoor ventilation air supplied to an indoor space. Specifically, we investigated the transfer of volatile organic compounds (VOCs) through the sandwiched membrane matrix ofthe ERV core, between two adjacent air streams. Pollutant transfer efficiency is calculated for experiments intentionally injecting two common indoor VOCs (acetone, isopropanol (IPA)) and the behavior of transfer is studied for different ERV exhaust and supply flowrates (supply, exhaust, balanced scenarios). Maximum pollutant transfer efficiency of 17% is recorded for isopropanol at balanced (equal supply and exhaust airflow rates) conditions at intake and exhaust air lines. Maximum pollutant transfer efficiency of 26% and a minimum of 5.3% for unbalanced CFM settings are obtained. For VOCs studies, we observed short response times of <10s from starting injection of VOCs into indoor exhaust air stream until the concentration at the indoor supply air stream reaches to steady state. This results concluded that, ERVs typically have a lower response time to pollutant re-entrainment.

KEYWORDS: Mass Transfer, Volatile Organic Compounds, Proton Transfer Reaction Mass Spectrometry (PTR-TOF), Indoor Air Quality (IAQ), Transfer Efficiency, Response Time Analysis, Pollutant Dynamics

I. INTRODUCTION

Indoor air quality (IAQ) is an important aspect for maintaining healthy lifestyles and reducing illnesses that are mainly related to the respiratory system [1], [2]. Previous studies reported that even at low levels of concentrations of pollutants, such as VOCs, particulate matter (PM) and carbon dioxide (CO2) at indoor space are associated with respiratory and other adverse health outcomes in occupants[2]. The best method to achieve a good IAQ is providing sufficient ventilation for the building space so far[3].

Among the multiple methods available to produce mechanical ventilation, energy recovery ventilators (ERVs) become a necessary device. ERVs help to extract heat and moisture from exhaust stale air streams and transfer them to supply fresh air streams by saving energy that is required for direct heating and humidification. Yang *et al.* [4] concluded that ERVs not only improves the IAQ but also reduce the building energy consumption by recording 34.56% efficiency, in a set of experiments they performed based on ERV in an indoor stadium. Among the few types of ERVs available for applications, membrane type ERVs are widely used due to their simplicity and versatility in operation[4].

While ERVs offer the opportunity for energy-efficient ventilation, prior studies indicate that mass transport of contaminants from the exhaust to supply airflow of ERVs are possible for an indoor burst of pollutants due to everyday operations[5]–[8]. The mass transport in ERVs is mainly assessed by the factor referred to as exhaust air

transfer efficiency (EATR)[5]. Hult *et al.*[5] performed experiments on rotary enthalpy ERV based on formaldehyde crossover to evaluate EATR value. The EATR calculation process introduced by studies [5]–[7] is related to the definition by ASHRAE. Hult *et al.*[5] found that the EATR values range from 10-29 % for a rotary enthalpy wheel, concluding that the bulk of the transfer is due to the air leakage from the wheel and 30% of the transfer process due to absorption and desorption. Patel *et al.* [6] performed studies in contaminant cross over in run around- membrane energy exchangers (RAMEE) using the same EATR parameter concept. They used toluene (C_7H_8) and formaldehyde (HCHO) as trace VOCs to test the re-entrainment. They have reported that EATR for toluene falls 2.3-3.4 % and 4.5-6.4 % for formaldehyde. Importantly, they have stated that there is a negligible transfer of low water-soluble VOCs (toluene), however, a detectable transfer from high water-soluble VOCs (formaldehyde) in RAMEE type ERV. Furthermore, for RAMEE's they found that EATR values are insensitive to changes in airflow rates, liquid desiccant flow rates, latent effectiveness and environmental conditions. Ryan *et al.* [7] reported EATR values observed by previous researchers in their paper. They used CONTAM software to model pollutant transfer rates under different permeabilities of the membrane material. In addition, Ryan *et al.* [7] performed experiments considering a single membrane by an experimental test rig fabricated to ASTM F-739 standard and their EATR values ranged from 0%-50%. Weerasekera and Laguerre[9] introduced a coupled continuum scale transport model for contaminant crossover in ERVs. Their simulations were based on microscopic aspects of contaminant transfer between a single membrane of an ERV. They used PTR-TOF MS data to validate their simulation results [9]. Further studies have been performed by Weerasekera and Cao [10] on contaminant diffusion in polymeric membranes which are widely utilized as a material for membrane cores in ERVs. They have proved the contaminant crossover behavior by applying multiple modelling approaches (Fick's diffusion, Darcy pore flow model, computational fluid dynamics) and arrived at convergence with all models which were used in study [10]. In this work, we expand on the above prior studies investigating VOC crossover in fixed membrane core ERVs adding another two important VOCs: acetone and isopropyl alcohol. These compounds are selected since they are ubiquitous and present at high variable concentrations in an indoor environment and not previously studied in literature [11]. Through this study, we have evaluated the EATR values for fixed membrane ERVs also studied the response behavior of membrane ERV to pollutant crossover to close this research gap.

II. MATERIALS AND METHODS

A. Experimental apparatus

We built an experimental setup using a residential-scale commercial ERV (Panasonic Intellibalance-100). The study was performed at the Department of Biochemistry and Molecular Biology of Oregon State University, Corvallis OR, USA from August 2019 to May 2021 using proton transfer reaction time of flight mass spectrometry (PTR-TOF) as the main concentration measurement instrument. The ERV has a maximum airflow rate of $100 ft^3/min$ and a minimum of $50\, ft^3/min$ for both intake and exhaust airlines with apossibility of $10 ft^3/min$ increments for both directions. The schematic of the experimental setup based on the ERV is shown in figure 1. Figure 2-a represents the real-time nomenclature of ERVs ports and airflow rates and figure 2-b shows the mass spectrometer (PTR-TOF-1000) that has been used for measurements. PTR-TOF. The ERV ports are named based on the flow at each port, e.g., the indoor exhaust air duct, where the air is taken from the indoor space, is named as I-Ex port. The port which is exhausting indoor air to the outdoor environment is named as O-Ex. The port which brings fresh air from outdoors is named as O-Supp. And finally, the port that supplies "fresh" air to the indoors is named I-Supp. Figure 1 represents this naming convention, which will be used in subsequent presentations and discussions of experimental results. The pollutant was injected into the I-Ex port of the ERV using the VOC generating set up as shown in Figure 3.

B. Transfer efficiency

Mass of the pollutant transported through each port of the ERV is based on calculating mass flux to the mass flow rate of the compound. By knowing the volumetric flow rate and concentrations at each port, mass flow rate M_x can be calculated as[8],

$$M_x = C_x . VFR_x \quad (1)$$

Where, C_x is the concentration measured at the x^{th} port of the ERV and VFR_x is the volumetric flow rate measured at the same port. By taking the concentration measurements from each ERV port, pollutant transfer efficiency can be calculated as,

$$EATR = \frac{M_{I-Supp} - M_{O-Supp}}{M_{I-Ex} - M_{O-Supp}} \quad (2)$$

In the above equation, both mass flow rates are normalized by an outdoor mass flow rate of the compound (M_{O-Supp}) to avoid the inconsistency due to the variation of outdoor compound concentration. Where subscript x is replaced by the port nomenclature as in Figure 1. For unbalanced CFM conditions, equation 2, can be simply multiplied with the

factor, Supply CFM/Exhaust CFM for convenience. This description can be represented mathematically as,

$$EATR = \frac{C_{I-Supp} - C_{O-Supp}}{C_{I-Ex} - C_{O-Supp}} \times \frac{VFR_{Intake}}{VFR_{Exhaust}} \quad (3)$$

Where, VFR_{Intake} is the intake line CFM value which is equal to VFR_{I-Supp} and VFR_{O-Supp}. And $VFR_{Exhaust}$ is the CFM of the exhaust line and it is equal to VFR_{I-Ex} and VFR_{O-Ex}. For a balanced CFM arrangement and $\frac{VFR_{Intake}}{VFR_{Exhaust}} = 1$, and for an unbalanced CFM arrangement $\frac{VFR_{Intake}}{VFR_{Exhaust}}$ takes a positive value.

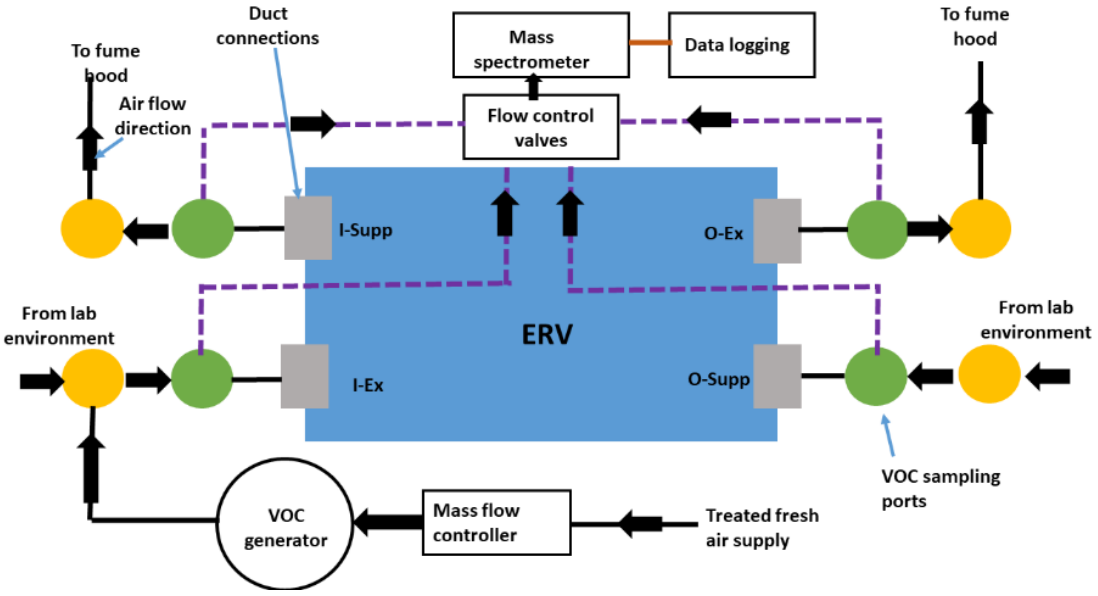

Figure 1: Schematic of the experiemntal setup and port nomenclature

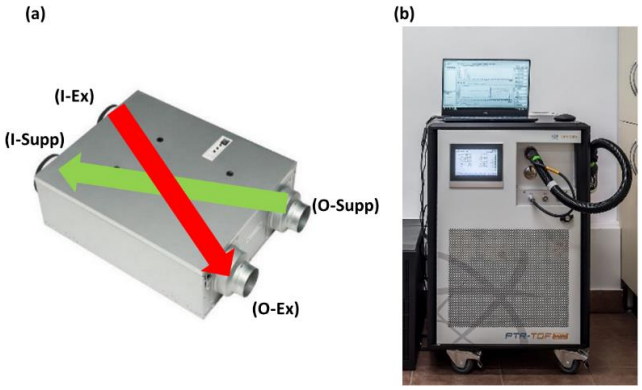

Figure 2: Real-time ERV port nomenclature and mass spectrometer

Panasonic Intellibalance 100 ERV and identification of airflow ports and airflow directions, (b). Ionicon analytik PTR-TOF-1000 MS

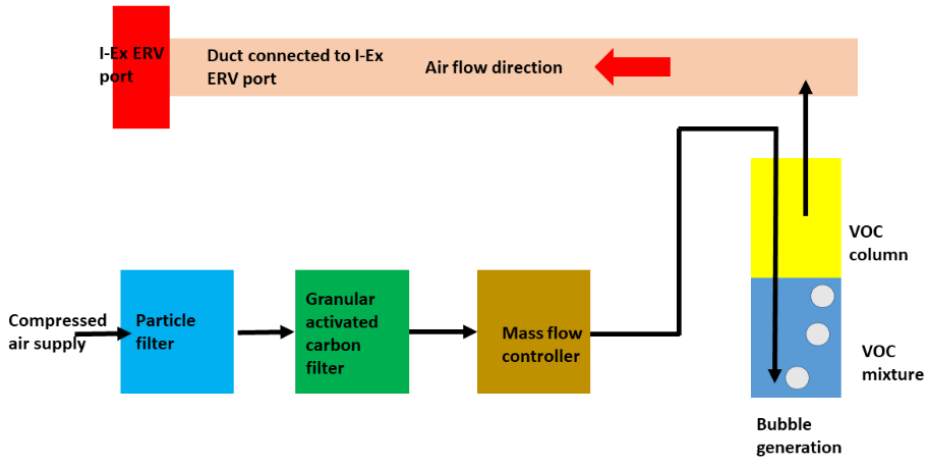

Figure 3: Schematic of the VOC generating setup and connection to I-Ex ERV port

C. Transfer efficiency

Mass of the pollutant transported through each port of the ERV is based on calculating mass flux to the mass flow rate of the compound. By knowing the volumetric flow rate and concentrations at each port, mass flow rate M_x can be calculated as[8],

$$M_x = C_x . VFR_x \quad (1)$$

Where, C_x is the concentration measured at the x^{th} port of the ERV and VFR_x is the volumetric flow rate measured at the same port. By taking the concentration measurements from each ERV port, pollutant transfer efficiency can be calculated as,

$$EATR = \frac{M_{I-Supp} - M_{O-Supp}}{M_{I-Ex} - M_{O-Supp}} \quad (2)$$

In the above equation, both mass flow rates are normalized by an outdoor mass flow rate of the compound (M_{O-Supp}) to avoid the inconsistency due to the variation of outdoor compound concentration. Where subscript x is replaced by the port nomenclature as in Figure 1. For unbalanced CFM conditions, equation 2, can be simply multiplied with the factor, Supply CFM/Exhaust CFM for convenience. This description can be represented mathematically as,

$$EATR = \frac{C_{I-Supp} - C_{O-Supp}}{C_{I-Ex} - C_{O-Supp}} \times \frac{VFR_{Intake}}{VFR_{Exhaust}} \quad (3)$$

Where, VFR_{Intake} is the intake line CFM value which is equal to VFR_{I-Supp} and VFR_{O-Supp}. And $VFR_{Exhaust}$ is the CFM of the exhaust line and it is equal to VFR_{I-Ex} and VFR_{O-Ex}. For a balanced CFM arrangement and $\frac{VFR_{Intake}}{VFR_{Exhaust}} = 1$, and for an unbalanced CFM arrangement $\frac{VFR_{Intake}}{VFR_{Exhaust}}$ takes a positive value.

D. Experimental protocol

From the various CFM settings possible for intake and exhaust air streams, we extracted the most significant CFM arrangements that can mainly be considered. Concentration measurements at each port are established according to these CFM settings. As a preliminary approach, to observe the pattern of VOC transfer efficiency, we performed our experimental matrix with equal, low difference and high difference CFM arrangements of exhaust and intake air streams. This matrix is shown in Table 1.

E. Maintaining mass balance closure

The measurements that are taken can be validated by analyzing the general mass balance of the compound for each CFM setting. Respectively, general mass balance can be performed as a derivative of equations 2 and 3 as follows,

$$M_{Sinked} = M_{I-Ex} - M_{O-Ex} \quad (3)$$

And,

$$M_{Sourced} = M_{I-Supp} - M_{O-Supp} \quad (4)$$

Table 1: Significance of balance and unbalanced CFM setting

CFM Setting (Exhaust Line/ Supply Line)	**Significance of the CFM Setting**
50/50 70/70 100/100	Equal CFM settings in both exhaust and supply streams from ascending order
50/100 100/50	High CFM difference in two streams
60/90 90/60	Medium CFM difference
70/80 80/70	Low CFM difference

III. RESULTS AND DISCUSSION

A. Transfer efficiencies

The transfer efficiency for each and individual CFM setting is calculated and compared by the concentration data which is obtained. Considering compound concentration, which is recorded as ppb from mass spectrometer software, is converted to mg/m^3 based on the molecular weights of acetone (59 g/mol) and IPA (60.1 g/mol) and CFM values are converted to m^3/s while applying to equation 1 for equal CFM conditions. The following efficiencies are computed by taking the average value of the fluctuating concentration for the sampling period and these average values are listed in the appendix. The error bars are developed under the methodology of the common error propagation method starting from the standard deviation of an individual measurement following the laws of arithmetic. Table 2 represents generalized EATR values obtained by previous researchers to provide context for the range of EATR values we report.

Table 2: Generalized EATR values recorded in the literature

Publication	EATR Value	Type of Device
Hult *et al.*[5]	10%-29%	Rotary enthalpy wheel
Patel *et al.*[6]	0%-6.4%	Run-around membrane type
Huizing *et al.*[7]	0%-50%	Membrane based ERV

Figures 4-6 represents the transfer efficiency (EATR) values for isopropyl alcohol through the ERV core. Also, when increasing the CFM conditions, the transfer efficiency of the compound is decreasing. One possible explanation for this occurrence is, flow velocities inside core channels are higher with higher CFM values, thus, the pollutant has less contact time with the membrane-air interfaces. Therefore, the pollutant is carried away from the flow to the exhaust port, reducing mass transfer across the membranes.

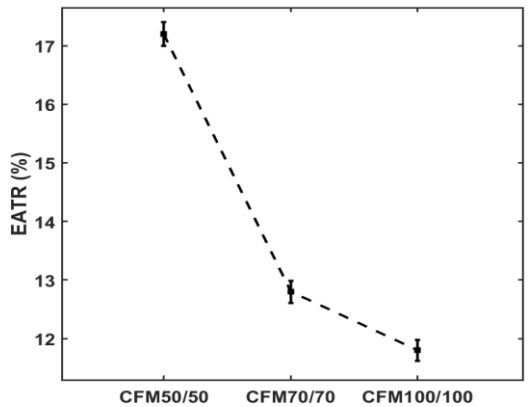

Figure 4: EATR values for balanced CFM settings for Isopropyl alcohol (C_3H_8O)

Unbalanced CFM condition-1 as introduced in Figure 5, is based on setting low CFM values in the exhaust line and high CFM values in the indoor supply line. The above plot is obtained for balanced and unbalanced CFM values for isopropyl alcohol satisfying the overall deviation of compound mass balance <5%. As the unbalanced settings approach balanced conditions, the EATR (compound transfer efficiency) values calculated approach to respective balanced conditions. For example, in setting 70/80, an EATR of 10.1% is measured, which is near to the EATR of the balanced CFM setting (70/70) of 12.8%. Under conditions with greater exhaust/inlet imbalance, higher compound transfer efficiency for IPA is recorded, with 26.2% of EATR at 50/100 CFM setting

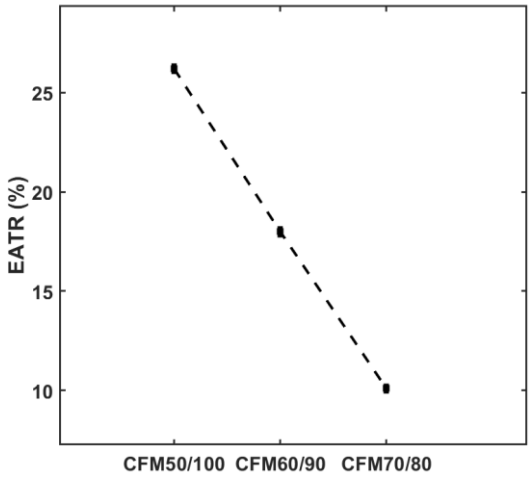

Figure 5: EATR values for unbalanced CFM settings as in condition 1 for Isopropyl alcohol (C_3H_8O)

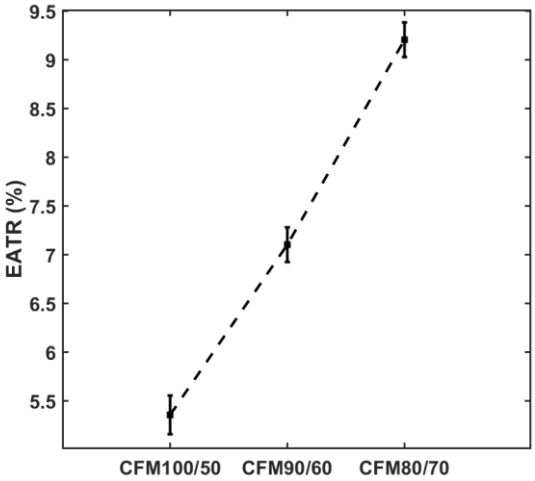

Figure 6: EATR values for unbalanced CFM settings as in condition 2 for Isopropyl alcohol (C_3H_8O)

When high CFM values are set for the exhaust line and low CFM values for the supply line, as in Figure 6, shows lower transfer efficiencies. The lowest EATR was recorded at

100/50 exhaust/supply airflow, at 5.35%. Again, as the imbalance between exhaust and supply is reduced, we observe an EATR that approaches respective imbalanced conditions (e.g., 80/70 results in an EATR of 9.2% vs 70/70 resulting in EATR of 12.8% (Figure 5)).

The behavior of the transfer efficiencies for unbalanced conditions can be successfully explained through species advection and diffusion theory, according to Weerasekera *et al.*[9], as they already introduced explanations related to membrane type ERVs based on this theory. For unbalanced CFM condition-1, relatively low CFM values increase the interface contact time of the compound with the membrane-air interface providing more opportunity for interface mass transfer at the exhaust side. Relatively high CFM values at the supply side have high advective currents and low static pressures compared to the exhaust side, providing positive pressure induced diffusion of the compound from the exhaust side to the supply side. It is entirely clear that the opposite phenomenon occurs at unbalanced CFMcondition-2 creating negative pressure induced diffusion from the exhaust to supply sides simultaneously creating lower transfer efficiencies.

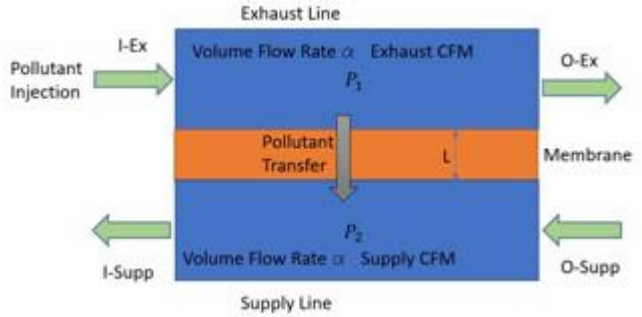

Figure 7: Microscopic depiction of the pollutant transfer process. Where, P_1 and P_2 are static pressures at the exhaust side andsupply side. L is the membrane thickness

A more detailed explanation of the behavior of the transfer process can be presented in Figure 7. Where, from the microscopic point of view, the development of the ERV membrane core can be simplified to a system containing two channels separated by a porous membrane. Under ideal balanced CFM conditions, static pressures at either side of the membrane can be approximated as equal based on equal airflow velocities at either side of the channel core channels. Therefore, the static pressure gradient across the membrane ($\Delta P = (P_1 - P_2)/L$) can be approximated to zero. In this type of setting, apart from the air leakage, the only pollutant transfer process is Fick's diffusion. For unbalanced CFM condition-1, the exhaust side has a higher static pressure and the supply side has a lower static pressure, therefore, $\Delta P > 0$ creates a pressure-induced diffusion process from the exhaust side to the supply side. On contrary, for unbalanced CFM condition 2, $\Delta P < 0$ is observable. Therefore, this negatively induced pressure gradient is reducing the diffusion process creating lower efficiencies of pollutant transfer.

B. Abnormality of entrainment of acetone

Transfer efficiencies in Ffigures 6-8 are computed for isopropyl alcohol where satisfactory mass balance with a deviation range <5%. Figures 8a-c and 9a-c represents one result of a typical experiment performed on acetone and isopropyl alcohol with balanced (50/50) and unbalanced (50/100) CFM conditions respectively. Figure 8b-c and 9b-c compare the results between isopropyl alcohol and acetone. Here,acetone-isopropyl alcohol mixture is injected into the I-Ex port and entrainment characteristics are observed. It is visible from the time series plot, that, acetone concentration at the I-Supp port has an unacceptably high value compared to its value at the exhaust port (I-Ex, O-Ex) (Figure 8b). However, isopropyl alcohol acts normally satisfying regular mass balance conditions. From this result, we hypothesize that there is a high absorption and emission rate for acetone in the membrane core and there can be a possibility of accumulation of this compound in the core. Furthermore, preliminary background concentration tests performed for acetone before each experiment confirmed that there is no late emission of acetone from the ERV core. This result is a topic for further evaluation under different research.

C. Response from the ERV for pollutant transfer

It is of utmost importance to study the reaction time of the ERV to pollutant transport. Therefore, this study is performed in two aspects. In the first case, continuous measurements are taken at the I-Supp port conforming compound concentration at this port that is at the laboratory VOC concentration. The pollutant is supplied afterwards and supply start time vs concentration variation at the I-Supp port is examined. From the same way concentration at the I- Supp port after stopping the VOC supply is also observed. Figure 10 presents the time series plots of raw measurements for three equal CFM settings (50/50, 70/70 and 100/100) in response time analysis and table 3 represents the overview of the response time experiments performed using isopropyl alcohol as the trace compound.

Table 3: Overview of the response time measured for equal CFM experiments extracted from time series plots considering both compounds

Time series plot	Injection start point	Injectionstopping point	Response time to achieve first concentration spike at I- Supp port	Response time to achieve steady ambient concentration at I- Supp port
Figure 10-a	79s	127s	7s	196s
Figure 10-b	116s	197s	8s	226s
Figure 10-c	85s	159s	10s	249s

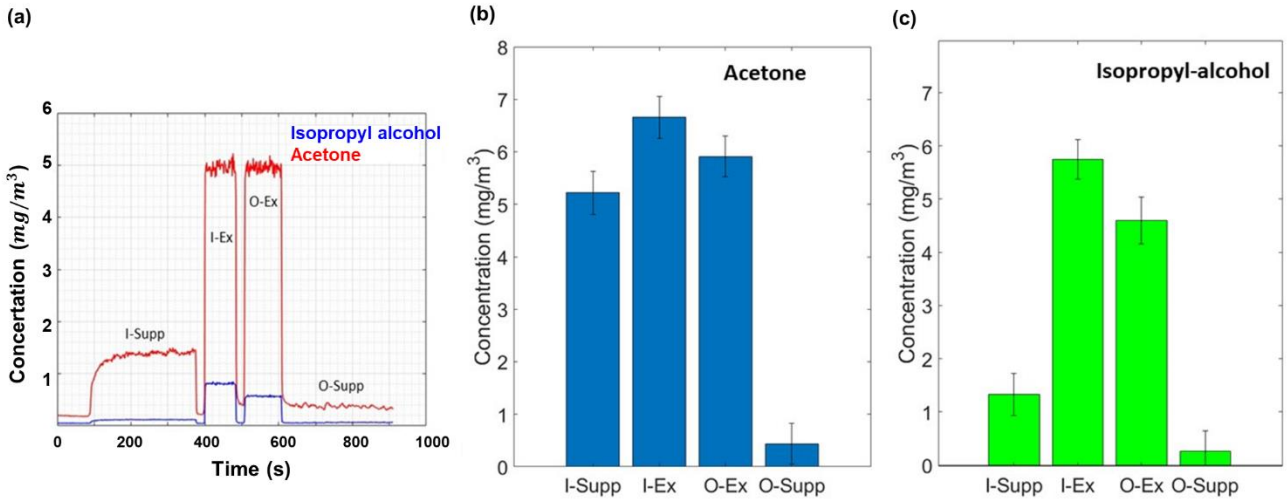

Figure 8a-c: Abnormality in crossover of acetone as a contaminant at balanced CFM conditions. (a) Time series plot for the experiment that was performed for 50/50 equal CFM setting (Spike identification is same as in figure 4), (b) Comparative bar graph for mean concentrations at each sampling port for same CFM setting (Note: Magnitude of concentration for each compound measured from the zero level for above bar graph)

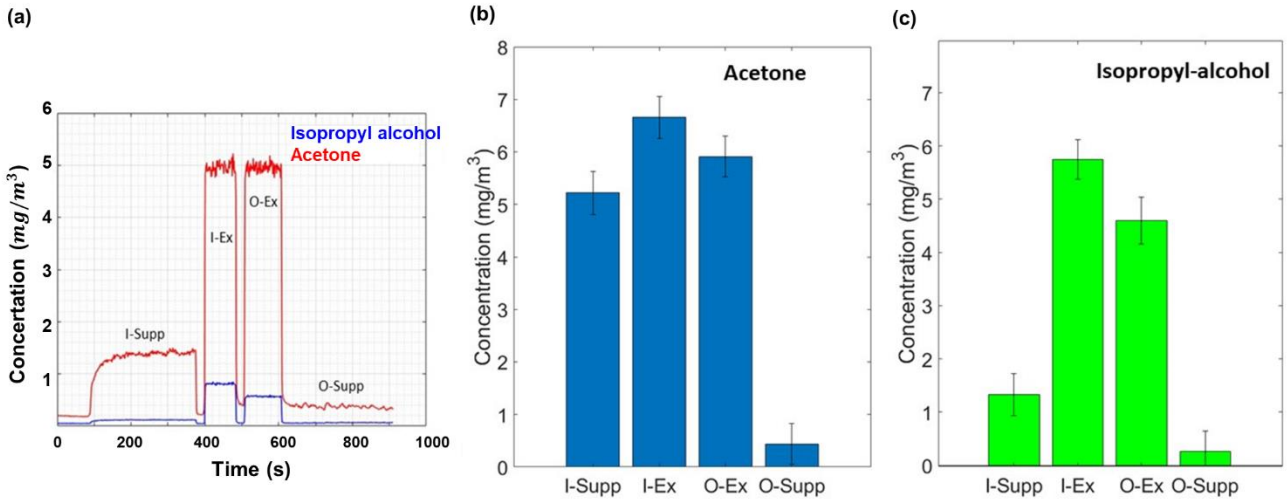

Figure 9a-c: Abnormality in crossover of acetone as a contaminant at unbalanced CFM conditions. (a): Time series plot for the experiment that was performed for 50/100 CFM setting (Spike nomenclature is same as in figure 4), (b): Comparative bar graph for the concentrations at each sampling port for same CFM setting (Note: Magnitude of concentration for each compound measured from the zero level for above bar graph)

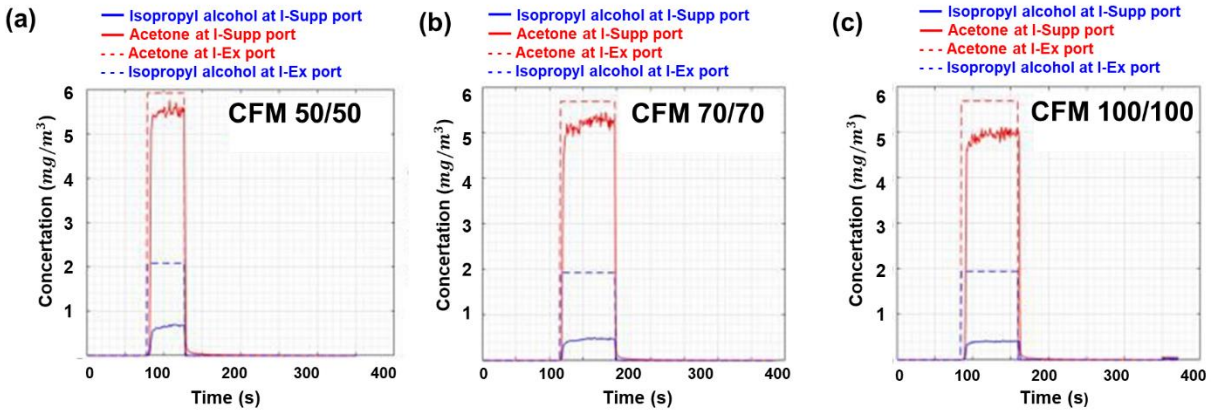

Figure 10a-c: ERV response time measurement process for trace compounds acetone and isopropyl alcohol. (a). Response analysis at 50/50 CFM setting, (b). Response analysis at 70/70 CFM setting and (c). Response analysis at 100/100 CFM setting

From the above results, it is evident that the device has relatively fast response times when considering re-entrainment start time from the beginning of VOC supply to the I-Ex port. The response time to reach the steady-state concentration of the compound after the start of supply can be averaged to <10s. The response is not instantaneous after cessation of injection, and there exists a lag before a return to steady-state conditions with the I-Ex concentration post-emission event. We hypothesize that the driver for this occurrence is the re-emission of absorbed compounds into the membrane matrix. Note that all these experiments are performed after conforming the concentrations of each ERV port is equivalent to laboratory VOC concentrations. Therefore, effects from outside factors, apart from VOC supply to the I-Ex port are avoided.

When comparing EATR values for fixed membrane based ERVs with rotary enthalpy wheels and run-around type ERVs, we can consider that fixed membrane based ERVs are more vulnerable for pollutant re-entrainment based on current study as well as from previous studies [5]–[7]. Current study shows a maximum EATR value of 26.2% which falls between predicted EATR range as presented by Huizing *et al.*[7]. By increasing the exhaust air flow rate compared to intake air flow rate, pollutant reentrainment can be significantly reduced due to increased advection currents in the exhaust line also by reducing membrane-air interface diffusion[9]. As the main implication from the study, in a typical practical fixed membrane ERV application, we recommend to operate an ERV in unbalanced conditions with high exhaust air flow rate and low intake air flow rate to reduce the impact from an indoor pollutant burst on occupants while still maintaining required fresh air supply rates.

IV. CONCLUSION

Contaminant crossover through residential energy recovery ventilators is studied through this work using isopropyl alcohol and acetone as the trace compounds. We observed that the minimum transfer efficiency (5.35%) is observed when ERV is operated under unbalanced CFM conditions with higher exhaust line CFM value compared to input line CFM. The highest transfer efficiency (26.2%) is observed when exhaust line CFM is a low value. Compared to the transfer behavior of isopropyl alcohol, acetone demonstrated an anomaly of transfer observing late emission from the ERV core resulted in increased crossover concentrations. We also conclude that membrane ERVs are highly vulnerable to contaminant crossover showing low response time to indoor related pollutant bursts.

V. SIGNIFICANCE STATEMENT

This study discovers the potential of contaminant crossover in membrane ERVs that can be beneficial for understanding the vulnerability of different membrane-type ERV designs and membrane materials for contaminant crossover. The current study also contributes to implementing remediation measures to reduce such contaminant crossover by efficient settings of intake and exhaust airflow rates of a typical membrane ERV. This study will help the researcher to uncover the critical areas of achieving better IAQ levels that can tremendously improve the occupant performance and health risks where critical research is necessary.

ACKNOWLEDGEMENT

Naveen Weerasekera, Ryan Martil, Dawa Shingdan and Agnimitra Biswas and Siyua Cao wish to thank Portland State Institute for Sustainability for funding this work. Naveen Weerasekera, Ryan Martil and Siyua Cao also pay gratitude to Nethmini Weerasekera for technical support on PTR-TOF mass spectrometry and Dr. Agnimitra Biswas, associate professor of National Institute of Technology-Silchar, India, for his constant advices in all thermal and fluid science aspects.

REFERENCES

1. A. Cincinelli and T. Martellini, "Indoor Air Quality and Health," *IJERPH*, vol. 14, no. 11, p. 1286, Oct. 2017, doi: 10.3390/ijerph14111286.
2. L. Zhong, F.-C. Su, and S. Batterman, "Volatile Organic Compounds (VOCs) in Conventional and High Performance School Buildings in the U.S.," *IJERPH*, vol. 14, no. 1, p. 100, Jan. 2017, doi: 10.3390/ijerph14010100.
3. J. T. Rosbach, M. Vonk, F. Duijm, J. T. van Ginkel, U. Gehring, and B. Brunekreef, "A ventilation intervention study in classrooms to improve indoor air quality: the FRESH study," *Environ Health*, vol. 12, no. 1, p. 110, Dec. 2013, doi: 10.1186/1476-069X-12-110.
4. P. Yang, L. Li, J. Wang, G. Huang, and J. Peng, "Testing for Energy Recovery Ventilators and Energy Saving Analysis with Air-Conditioning Systems," *Procedia Engineering*, vol. 121, pp. 438–445, 2015, doi: 10.1016/j.proeng.2015.08.1090.
5. E. L. Hult, H. Willem, and M. H. Sherman, "Formaldehyde transfer in residential energy recovery ventilators," *Building and Environment*, vol. 75, pp. 92–97, May 2014, doi: 10.1016/j.buildenv.2014.01.004.
6. H. Patel, G. Ge, M. R. H. Abdel-Salam, A. H. Abdel-Salam, R. W. Besant, and C. J. Simonson, "Contaminant transfer in run-around membrane energy exchangers," *Energy and Buildings*, vol. 70, pp. 94–105, Feb. 2014, doi: 10.1016/j.enbuild.2013.11.013.
7. Ryan Huizing, Hao Chen, Frankie Wong, "Contaminant transport in membrane-based energy recovery ventilators," *Science and Technology for the Built Environment*, no. 21, pp. 54–66, 2015.
8. C. Boardman and S. V. Glass, "Moisture transfer through the membrane of a cross-flow energy recovery ventilator: Measurement and simple data-driven modeling," *Journal of Building Physics*, vol. 38, no. 5, pp. 389–418, Mar. 2015, doi: 10.1177/1744259113506072.
9. N. D. Weerasekera and A. Laguerre, "Coupled Continuum Advection-Diffusion Model for Simulating Parallel Flow Induced Mass Transport in Porous Membranes,", "International Journal of Science and Research" vol. 8, no. 12, p. 7, 2019, pp 694-700. DOI: 10.21275/ART20203395
10. N. D. Weerasekera and S. Cao, "Multifaceted Convergence Study for Evaluating Gas Diffusion Parameters of Polymeric Membranes," *IJEAS*, vol. 6, no. 11, Nov. 2019, pp 57-63, doi: 10.31873/IJEAS.6.11.21.
11. K. K. W. Tang and M. R. Mahmud, "The Accuracy of Satellite Derived Bathymetry in Coastal and Shallow Water Zone," *Int J. of BES*, vol. 8, no. 3, pp. 1–8, Aug. 2021, doi: 10.11113/ijbes.v8.n3.681